HHS Public Access

Author manuscript

Biochim Biophys Acta. Author manuscript; available in PMC 2019 August 01.

Published in final edited form as:

Biochim Biophys Acta. 2018 August ; 1864(8): 2538–2549. doi:10.1016/j.bbadis.2018.05.008.

Axed MUC4 (MUC4/X) aggravates pancreatic malignant phenotype by activating integrin-β1/FAK/ERK pathway

Rahat Jahan[a], **Muzafar A. Macha**[a,b], **Satyanarayana Rachagani**[a], **Srustidhar Das**[a], **Lynette M. Smith**[c], **Sukhwinder Kaur**[a], and **Surinder K. Batra**[a,d,*]

[a]Department of Biochemistry and Molecular Biology, Fred and Pamela Buffett Cancer Center, University of Nebraska Medical Center, NE-68198, USA

[b]Department of Otolaryngology-Head and Neck Surgery, Fred and Pamela Buffett Cancer Center, University of Nebraska Medical Center, NE-68198, USA

[c]Department of Biostatistics, Fred and Pamela Buffett Cancer Center, University of Nebraska Medical Center, NE-68198, USA

[d]Eppley Institute for Research in Cancer and Allied Diseases, Fred and Pamela Buffett Cancer Center, University of Nebraska Medical Center, NE-68198, USA

Abstract

Alternative splicing is evolving as an eminent player of oncogenic signaling for tumor development and progression. Mucin 4 (MUC4), a type I membrane-bound mucin, is differentially expressed in pancreatic cancer (PC) and plays a critical role in its progression and metastasis. However, the molecular implications of MUC4 splice variants during disease pathogenesis remain obscure. The present study delineates the pathological and molecular significance of a unique splice variant of MUC4, MUC4/X, which lacks the largest exon 2, along with exon 3. Exon 2 encodes for the highly glycosylated tandem repeat (TR) domain of MUC4 and its absence creates MUC4/X, which is devoid of TR. Expression analysis from PC clinical samples revealed significant upregulation of MUC4/X in PC tissues with most differential expression in poorly differentiated tumors. *In vitro* studies suggest that overexpression of MUC4/X in wild-type-MUC4 (WT-MUC4) null PC cell lines markedly enhanced PC cell proliferation, invasion, and adhesion to

*Corresponding author at: Department of Biochemistry and Molecular Biology, University of Nebraska Medical Center, Omaha, NE 68198-5870, USA. sbatra@unmc.edu (S.K. Batra).

Supplementary data to this article can be found online at https://doi.org/10.1016/j.bbadis.2018.05.008.

Transparency document

The Transparency document associated this article can be found, in online version.

Disclosure of potential conflicts of interest

No potential conflicts of interest were disclosed.

Contributions

Rahat Jahan: Designed and performed experimental methods (*in vitro* and *in vivo* studies), cloning, and expression of inducible MUC4/X construct, analysis, and interpretation of the data, and wrote the manuscript.
Muzafar A. Macha: Designed, performed, analyzed and interpreted the data, scientific adviser and critically revised the manuscript.
Satyanarayana Rachagani: Orthotopic transplantation study, and critically revised the manuscript.
Shrustidhar Das: Cloning and expression of MUC4/X construct. Lynette Smith: Statistical analyses.
Sukhwinder Kaur: Interpretation of data, scientific adviser, and critically revised the manuscript.
Surinder K Batra: Supervised the work, study concept and design of the study, critically reviewed, and edited the manuscript. All authors read and approved the final manuscript.

extracellular matrix (ECM) proteins. Furthermore, MUC4/X over-expression leads to an increase in the tumorigenic potential of PC cells in orthotopic transplantation studies. In line with these findings, doxycycline-induced expression of MUC4/X in an endogenous WT-MUC4 expressing PC cell line (Capan-1) also displayed enhanced cell proliferation, invasion, and adhesion to ECM, compared to WT-MUC4 alone, emphasizing its direct involvement in the aggressive behavior of PC cells. Investigation into the molecular mechanism suggested that MUC4/X facilitated PC tumorigenesis *via* integrin-β1/FAK/ERK signaling pathway. Overall, these findings revealed the novel role of MUC4/X in promoting and sustaining the oncogenic features of PC.

Keywords

Pancreatic cancer; MUC4; MUC4/X; Splice isoform; Tumorigenesis; Metastasis

1. Introduction

Pancreatic cancer (PC) is the third leading cause of cancer-related deaths in the USA and is predicted to become second by 2030 [1,2]. Due to high complexity and degree of heterogeneity, the molecular mechanisms for progression and early metastasis remain obscure. Alternative splicing is one of the mechanisms that contributes to the complexity and effectiveness of disease progression; therefore, it stands to reason that cancer cells adopt alternative splicing to sustain themselves within a hostile environment. Recently, alternative splicing has gained immense attention in cancer research due to its strong association with tumor development as well as an attractive anticancer therapeutic target(s) [3]. For example, splice variant of the CD44 adhesion molecule has been implicated in the metastatic spread of various human tumor cells and has been correlated with poor prognosis [4]. Another example of a well studied oncogenic splice variant in PC, is the paired related homeodomain transcription factor (PrrX1). Two alternative isoforms of PrrX1 (PrrX1a, and PrrX1b) have shown distinct but complementary roles in PC oncogenesis [5]. Prrx1b regulates epithelial to mesenchymal transition (EMT) which promotes invasion, while Prrx1a regulates mesenchymal to epithelial transition (MET) by tumor redifferentiation which enhances metastatic colonization [5]. All these previous studies suggest that splice variants have distinct and pronounced functions at different stages of tumor progression, and therefore further exploration is merited for delineating their mechanistic and therapeutic significance in a highly lethal malignancy like PC.

The type 1 transmembrane mucin MUC4, is one of the most differentially overexpressed genes in PC, with undetectable expression in normal pancreas and *de novo* expression in early precursor lesions [6]. With this differential expression in PC, MUC4 has been implicated as a primary oncogenic player with prominent roles in neoplastic transformation, tumor progression, metastasis, and chemoresistance [7–11]. It is comprised of 26 exons organized into unique domains including a variable tandem-repeat (TR) domain, nidogen-like (NIDO) domain, adhesion-associated domain in MUC4 and other proteins (AMOP), three EGF-like domains (EGF), transmembrane (TM) domain and a short cytoplasmic tail (CT) domain (Fig. 1a–b) [12,13]. We and others have identified 24 distinct variants of MUC4, however the functional implications of these splice variants in PC pathogenesis is

not fully elucidated [14]. Specifically, deletion of exons 2 and 3 results in the formation of MUC4/X, and deletion of exon 2 alone results in MUC4/Y [14]. Exon 2 codes for the largest domain of MUC4 and characteristic mucin structural signature defined by a TR region made of 145–500 repeats of 16 amino acids that are heavily *O*-glycosylated on serine and threonine residues [13].

Few mucin splice variants have been studied to assess their various pathological implications. Among them, the role of MUC1 splice variants have been studied in cancer and inflammatory diseases [15]. Previous research has shown that MUC1/Y is overexpressed in breast cancer patient tissues compared to normal adjacent tissues [16]. Additionally, overexpression of MUC4/Y has been associated with PC tumorigenesis by activating the JNK and AKT signaling pathways [17]. Also in PC patients, MUC4/Y overexpression is positively correlated with tumor invasion and metastasis [18].

Various transmembrane mucins, including MUC1 and MUC4, have been shown to impart steric hindrance to cell-ECM interaction due to their large glycosylated TR domain [19–21]. Further, it has been demonstrated that a higher number of tandem repeats in SMC/Muc4, the rat homolog of human MUC4, contributes to decreased adhesion of cancerous cells to the ECM protein fibronectin, suggesting that not only the presence, but extent of the TR region, is also responsible for adhesive properties [22]. Earlier studies from our group have also demonstrated the involvement of WT-MUC4 in impeding PC cells interaction with ECM by interfering with integrin-mediated cell adhesion [19]. These studies suggest a critical role of TR domain of WT-MUC4 for cell - ECM adhesion in PC pathogenesis.

The present study explores the molecular and pathological significance of MUC4/X in the pathogenesis of PC. Overall, our studies revealed significant expression of MUC4/X in PC tissues. Our studies also showed that overexpression of MUC4/X in PC cells augmented cell proliferation, invasion and metastasis in both *in vitro* and *in vivo* models. These effects were mediated by boosting the integrin-β1/FAK/ERK signaling pathway.

2. Methods & materials

2.1. Clinical samples

Pancreatic tumor tissues and adjacent normal tissues were obtained from the University of Nebraska Medical Center (UNMC) rapid autopsy program (RAP). The study was approved by the Institutional Review Board (IRB) at UNMC, and all participants were consented before tissue collection (IRB-091-01). Tumors were flash frozen in liquid nitrogen and stored at −80 °C until analysis.

2.2. RNA isolation from cell and frozen tissue, reverse transcription and real-time PCR

Total RNA from cells and frozen tissues were isolated using a mirVana miRNA kit (Ambion, Austin, TX, USA). RNA was reverse transcribed by using 1 μg of total RNA with random hexamer oligos (500μg/ml), 1 μl of 10 mM dNTPs, 5× first-strand reverse transcriptase buffer, 1 μl of 0.1 M dithiothreitol and 1 μl of (50 unit) SuperScript RT as described previously [8]. Briefly, 10 ng of complementary DNA was amplified using LightCycler® 480 SYBR Green I master mix (Roche Diagnostics, IN, USA) in the Light Cycler 480II

(Roche Diagnostics, IN, USA). The amplification was performed in a two-step cyclic process (95 °C for 5 min, followed by 45 cycles of 95 °C for 10 s, 60 °C for 10 s and 72 °C for 10 s). The relative expression of mRNA (ΔCt) was normalized with β-actin, and the relative fold change (ΔΔCt) was measured in reference to a normal human pancreatic ductal epithelial (HPDE) cell line. The WT-MUC4 and MUC4/X expression in clinical samples were analyzed and expressed as fold change (log10 transformed) relative to control group (HPDE). The qPCR primers used are listed in Supplementary Table S1.

2.3. Cell lines

MIAPaCa, Capan-1, AsPC-1 and CD18/HPAF PC cell lines were obtained from ATCC, and grown in Dulbecco's Modified Eagle's medium (DMEM) containing high glucose (Hyclone, Thermo USA), supplemented with 10% (v/v) fetal bovine serum and 1% penicillin-streptomycin (HyClone, Thermo, USA) at 37 °C in a humidified atmosphere containing 5% CO_2. Human mesothelial LP9/TERT-1 cells, an hTERT-immortalized cell line phenotypically and functionally resembling normal human peritoneal mesothelial cells, were obtained from Dr. James Rheinwald (Brigham and Women's Hospital, Harvard Institute of Medicine, Boston, MA) and cultured as detailed previously [23].

2.4. Generation and expression of MUC4/X construct

Standard PCR and molecular cloning techniques were utilized to generate MUC4/X overexpression constructs as detailed previously [24]. Briefly, the MUC4/X was amplified by RT-PCR from our miniMUC4 construct, cloned into the mammalian expression vector p3X-FLAG-CMV9 (Sigma-Aldrich, St. Louis, MO, USA) [25] and verified by sequencing. MIAPaCa and AsPC-1 PC cells were stably transfected using lipofectamine (Invitrogen, CA, USA) and stable clones were selected using G418 (400 μg/ml). Cells were analyzed for MUC4/X protein expression by immunoblotting and immunofluorescence using anti-FLAG antibody (1:3000, M2 clone, Sigma-Aldrich).

2.5. Generation of Teton inducible system

The DNA fragment encoding MUC4/X was amplified by RT-PCR from the p3X-FLAG-CMV9-MUC4/X construct and subcloned into a Topo 2.1 cloning vector using TOPO TA Cloning® kit (Invitrogen, CA, USA). Using *Sal*I and *Spe*I restriction digestion enzymes, the desired MUC4/X DNA fragment was digested from the Topo-TA, cloned into pTet-Splice vector (Invitrogen, CA, USA) and sequenced. Tetracycline-inducible MUC4/X expressing PC cell line Capan-1 was generated as detailed previously [26]. Briefly, Capan-1 cells were transduced with rtTA lentiviral particles according to the manufacturer's recommendations (Gentarget, Inc., CA, USA) and stably transfected clones were selected using puromycin (2 μg/ml). Subsequently, these rtTA transduced stable Capan-1 cells were transfected with pTet-Splice-MUC4/X plasmid, and after 48 h of transfection, MUC4/X expression was induced using doxycycline (2 μg/ml). MUC4/X expression was confirmed by performing immunoblotting and immunofluorescence using anti-FLAG antibody.

2.6. Cell proliferation assay (MTT assay)

The effect of MUC4/X overexpression on the viability/proliferation of PC cells was determined using MTT (3-[4, 5-dimethylthiazol-2-yl]-2, 5 diphenyl tetrazolium bromide) assay as described previously [27]. PC cells (MIAPaCa and AsPC-1) with an empty vector (MIAPaCa-EV and AsPC-1-EV) as control and MUC4/X over expressed MIAPaCa-MUC4/X and AsPC-1-MUC4/X cells (5×10^3/well) were seeded in triplicates onto a 96-well plate for 24–96 h in the presence of 2% serum containing media. Cell viability was assessed by adding 10 μl of 5 mg/ml of MTT in each well containing 90 μl of media (final working concentration of MTT is 0.5 mg/ml) followed by incubation for 3–4 h at 37 °C. 100 μl of dimethyl sulphoxide (DMSO) was added to dissolve formed formazan crystals. Optical density (OD) was measured at a wavelength of 450 nm and data collected was analyzed using the SOFTMAX PRO software (Molecular Devices Corp., Sunnyvale, CA, USA).

2.7. Ethynyl-2-deoxyuridine (EdU) incorporation assay

To assess the cell proliferation, control and MUC4/X overexpressing (MUC4/X-OE) cells (1×10^6/ml) were seeded in six-well plates onto the sterilized coverslip and analyzed for incorporation of 10 μM EdU (5-ethynyl-2′-deoxyuridine) using Click-iT EdU Cell Proliferation Assay Kit (Click-iT EDU kit, Thermo Fisher Scientific, MA, USA). Briefly, after incubating the cells with 10 μM of EdU for 24 h under dark conditions, cells were washed thrice with PBS, fixed with 4% paraformaldehyde and permeabilized with 0.1% Triton X-100 in PBS. The cell nuclei were stained with DAPI (4′, 6-Diamidino-2-Phenylindole, Dihydrochloride, Sigma-Aldrich, St. Louis, MO, USA) and visualized under a Zeiss confocal laser-scanning microscope (Carl Zeiss Microimaging, Thornwood, NY, USA). Percentage of proliferative cells were calculated by the number of EdU positive cells per field/total number of DAPI positive cells per field (*100).

2.8. Colony formation assay

500 cells/well were seeded in triplicate in a 6 well plate in 2% FBS containing medium [27]. After 2 weeks, cells were fixed with 100% methanol, stained with 0.4% crystal violet, and colonies were counted [27].

2.9. Western blotting

Western blotting was performed as described previously [27]. PC cells in log phase were lysed with ice-cold RIPA (50 mM Tris-HCl, 150 mM NaCl, 1% NP-40, 0.5% sodium deoxycholate and 0.1% SDS) containing protease and phosphatase inhibitors. Cell lysates were quantified, and equal amount of proteins were resolved on 8–12% SDS-PAGE (for < 250 kDa molecular weight proteins) and 2% agarose gel electrophoresis (for high molecular weight MUC4) and transferred onto polyvinylidene difluoride (PVDF) membranes. Membranes were blocked with 5% nonfat milk in phosphate-buffered saline (PBS) for 2 h, followed by incubation with primary antibodies at 4 °C overnight. Antibodies used includes: anti-FLAG (1:3000; Clone-M2, Sigma-Al-drich), MUC4 (In-house generated, 1:1000), β-actin (1:5000, Sigma-Aldrich), integrin-β1 (1:1000, Cell Signaling), phospho-ERK (1:1000, Cell Signaling), FAK (1:500, Santa Cruz Biotechnology), p-FAK (1:1000, Cell Signaling), HA (1:2000, Cell Signaling), total ERK (1:1000, Cell Signaling). After overnight

incubation, membranes were washed (3 × 10min in each time) and probed with appropriate secondary antibodies (1:10000) for 1 h at room temperature. The protein of interest was detected by enhanced chemiluminescence (Thermo Fisher Scientific, MA, USA). Protein levels were normalized with β-actin to determine fold changes using ImageJ software (version 1.50i, NIH).

2.10. Immunofluorescence

Immunofluorescence analysis was performed as detailed previously [27]. PC cells were grown to 60–70% confluency on sterilized cover-slips, washed with Hanks buffer, and fixed in ice-cold methanol for 2 min. Fixed cells were then blocked with 10% goat serum for 30 min at room temperature followed by incubation with primary anti-FLAG antibody (1:200) for 60 min at room temperature. After three consecutive washings with PBST, cells were incubated with Alexa Fluor-conjugated secondary antibody (1:200) for 60 min at room temperature. Cells were then washed with PBST (three times and 10 min in each time) and mounted using anti-fade vectashield mounting medium (Vector Laboratories Inc., Burlingame, CA, USA). Immunofluorescence was observed under Zeiss confocal laser-scanning microscope (Carl Zeiss Microimaging, Thornwood, NY, USA).

2.11. Invasion assay

Invasion assay was carried as described previously [8]. Briefly, six-well cell culture inserts were coated with Matrigel (BD Biosciences, Bedford, MA). Next, 5×10^5 cells/well were seeded on top of the chamber in triplicate, in serum-free media. Serum-containing medium was added to the lower chamber of the well. After 24 h, non-invaded cells were removed using cotton swabs, and cells that invaded into the lower side of insert were fixed, stained, and photographed (Dade-Behring Inc., Newark, DE 19714, USA). Photographs were taken from 5 random fields from each insert to count numbers of invaded cells per area. The experiment was repeated at least three times.

2.12. Wound healing assay

Wound healing assay was performed as per the standard protocol described previously [28]. Control and MUC4/X–OE cells were seeded at a density of 2×10^6 cells/well in six-well plate in growth medium and allowed to reach ~90% confluency. After 24 h, an artificial wound was created on the monolayer of the cells using a 200 μl sterile pipette tip, washed with PBS to remove damaged and detached cells and allowed the cells to migrate in 2% serum containing media. Images of control and MUC4/X-OE cells were taken at 0, 12 and 24 h and percentage of the wound closure was determined by the percentage of the ratio of wound width at 24 h to the wound width at 0h. The experiment was repeated thrice.

2.13. Adhesion assay

Adhesion assay was performed using Millicoat extracellular matrix (ECM) screening kit (#ECM 205 Millipore, Massachusetts, USA) which includes 96 well plate precoated with ECM proteins such as collagen I, collagen IV, fibronectin, vitronectin, and laminin. Control and MUC4/X-OE cells (2×10^5 cells/well) were plated in each well and allowed to attach for 5 h at 37 °C. Shorter incubation time (5 h) was chosen to avoid variations that arise due

to differential growth kinetics. Floating cells were carefully aspirated, and plates were washed with PBS. Attached cells were stained using crystal violet (0.1%, w/v in acetone) and solubilized using 200 μl of DMSO. Absorbance (at 570 nm) was measured using a microplate reader and data was analyzed using the SOFTMAX PRO software (Molecular Devices Corp., Sunnyvale, CA). Adhesion assays was performed twice in triplicate.

2.14. Mesothelial peritoneal cell adhesion assay

Adhesion of control and MUC4/X-OE cells to a monolayer of peritoneal mesothelial cells (LP9/TERT-1) was done as previously described [29]. Briefly, 2×10^4 LP9/TERT-1 cells per well were plated in flat-bottom 96-well plates and allowed to grow to a confluent monolayer for 48 h. Control and MUC4/X-OE cells were trypsinized, washed with PBS, and probed with 5 μmol/liter cell tracker green fluorescent CMFDA dye (Thermo Fischer Scientific, MA, USA) for 30 min at 37 °C. CMFDA labeled cells were washed with M199 medium with 0.1% fetal bovine serum to remove the free dye. Control and MUC4/X-OE cells were added (3×10^4 cells/well) onto the top of the monolayer of mesothelial cells. After 4 h incubation at 37 °C, total fluorescence in each well was recorded in a spectrofluorimeter (Perkin-Elmer, Turku, Finland) using 485-nm and 535-nm wavelengths for excitation and emission, respectively. Then, nonadherent cells were removed by gentle washing, followed by measurement of fluorescence. To calculate percentage of bound cells, values recorded for bound cells were compared with total fluorescence from cells before washing [30]. This assay was repeated twice in triplicates each time.

2.15. In vivo tumorigenesis and metastasis assay

Mouse orthotopic implantation experiments were performed under a protocol approved by the Institutional Animal Care and Use Committee (IACUC). Four to six-week-old athymic nude mice (equal number of males and females, housed separately) were purchased and maintained as described previously [8,24]. Briefly, after anesthetizing the mice by intraperitoneal administration of 120 mg/kg ketamine and 16 mg/kg xylazine, exponentially growing MIAPaCa-EV and MIAPaCa-MUC4/X cells (2.5×10^5 cells/50 μl of PBS) were orthotopically implanted into the head of the pancreas (vector control, n = 7, and MUC4/X, n = 8) [8]. To evaluate tumor growth and metastasis, mice were sacrificed by CO_2 asphyxiation and autopsied on the 50th day after implantation of tumor cells. After inspection of macroscopic tumor growth, the pancreas was resected and weighed. Both primary tumors and organs with metastases were kept in 10% formalin for 48 h followed by embedding in paraffin blocks. Blocks were cut into 0.5 μM-thick sections and processed for histochemical analysis.

2.16. H&E and immunohistochemical (IHC) staining

Tissues sections were stained with hematoxylin and eosin (H&E), and IHC was done using anti-FLAG (1:200, Sigma-Aldrich), anti-Ki67 (1:200, Cell Signaling Technology), anti-integrin-β1 (1:300, Cell Signaling Technology) antibodies as described previously [31].

2.17. Microarray gene expression analysis

Total RNA was isolated using the mirVana miRNA kit (Ambion, Austin, TX, USA). RNA yield and purity were measured using a Nanodrop (NanoDrop 1000 spectrophotometer, Thermo Scientific, Delaware USA). Affymetrix microarray was used to identify differentially expressed genes between MIAPaCa-EV and MIAPaCa-MUC4/X cells. Whole genome gene expression profiles were determined by the Microarray Core Facility at the University of Kansas Medical Center (UKMC, USA) using Human Gene 2.0 ST arrays (Affymetrix, Santa Clara, CA, USA). Target preparation, library labeling, hybridization, post-washing, and signal scanning were performed according to the protocol by UKMC. Microarray data were analyzed using Affymetrix Power software. Ingenuity pathway analysis (IPA) (QIAGEN, Valencia, CA, US) was performed to define canonical pathway differences between control and MUC4/X-OE PC cells and generate networks.

2.18. Statistical analysis

Statistical analysis was performed using Medcalc for Windows version 9.6.4.0 software (MedCalc Software, Mariakerke, Belgium) for analyzing patient data. Statistical differences between two groups was analyzed using unpaired, two-tailed *t*-test. The quantification is shown as the mean ± SD for *in vitro* studies where statistics refer to technical replicas denoted by “n”.

3. Results

3.1. Aberrant expression of MUC4/X in PC tumor tissues

The expression of WT-MUC4 and MUC4/X was investigated in normal pancreatic tissue adjacent to pancreatic tumor (NAT) (n = 8) and PC patient tissues [well-differentiated (WD, n = 7), moderately-differentiated (MD, n = 9), and poorly-differentiated (PD, n = 10)]. For MUC4/X expression assessment, the qPCR forward primer was designed to bind the junctional sequence of exons 1 and 4, and the reverse primer to bind the 3′ end of exon 4 (Supplementary Table S1). We observed significant upregulation of MUC4/X expression in PC samples compared to NAT samples ($p < 0.005$) (Fig. 1c). Interestingly, we also observed significantly high MUC4/X expression in PD tissues, compared to the NAT and WD tissues (NAT *vs.* PD, $p < 0.005$; WD *vs.* PD, $p < 0.001$) (Fig. 1d). We observed that all NAT tissues showed lower level of MUC4/X with a consistent elevated level WT-MUC4 expression as seen in Fig. 1e. While all the PC tissues displayed WT-MUC4 expression, 20% of WD, 40% of MD, and 80% of PD tumors showed higher expression of MUC4/X suggesting the WT-MUC4 and splice variant may complement each other in PC progression. Overall, deregulated expression of MUC4/X was observed in PC patient tissues (Fig. 1e and Supplementary Fig. S1a). Considering the significant overexpression of MUC4/X in PC, we next focused on delineating its pathobiological significance in PC tumorigenesis.

3.2. Overexpression of MUC4/X enhanced the cell proliferation and clonogenicity of PC cells in vitro

We examined the expression of MUC4/X in immortalized pancreatic cells in addition to the panel of PC cell lines with differential differentiation status. While no expression was

observed in immortalized normal pancreatic cell line HPDE, varied expression of MUC4/X were observed in PC cell lines with the lowest expression in MIAPaCa and SW-1990 and highest expression in BxPC3 cells (Supplementary Fig. S1b). Among these, MIAPaCa, PANC-1 and AsPC-1 cell lines do not express WT-MUC4 endogenously while Capan-1, BxPC-3, HPAC, and HPAF-II PC cell lines express moderate to high levels of WT-MUC4 (Supplementary Fig. S1b) [32]. To investigate the functional attributes of MUC4/X, stable overexpression of MUC4/X was carried out in MIAPaCa and AsPC-1 cells that do not express WT-MUC4 at the protein level, and have very low level of expression at the mRNA level (Supplementary Fig. S1b). It is worth mentioning, due to lack of antibodies for detecting MUC4/X protein, we generated a dual epitope-tagged MUC4/X mammalian expression construct, with N-terminal FLAG-tag and a C-terminal HA-tag (Supplementary Fig. S2a). The empty vector transfected cell lines (MIAPaCa-EV/AsPC-1-EV) were used as controls. Expression of MUC4/X was verified by immunoblot and immuno-fluorescence analyses, using anti-FLAG and anti-HA antibodies (Fig. 2a and Supplementary Fig. S2b). Additionally, our qPCR analysis also revealed almost no expression of WT-MUC4 in MIAPaCa-MUC4/X and AsPC-1-MUC4/X cells when compared to CD18/HPAF PC cell line (CD18/HPAF is a well-differentiated, highly aggressive and metastatic PC cell line) which expresses high levels of endogenous WT-MUC4 (Supplementary Fig. S2c) [33]. MTT assay revealed significant enhancement of cellular proliferation in MIAPaCa-MUC4/X and AsPC-1-MUC4/X cells compared to control cells at 3rd and 4th day time points (Fig. 2b). Consistent with MTT assay results, EdU incorporation assay also showed a significantly higher percentage of EdU positive MUC4/X-OE cells compared to control cells ($p < 0.05$) (Fig. 2c). As shown in Fig. 2d, we also observed that overexpression of MUC4/X significantly increased colony forming ability of MIAPaCa-MUC4/X and AsPC-1-MUC4/X cells ($p < 0.005$) as compared to control cells. Together, these findings support the notion that MUC4/X promotes proliferation of PC cells.

3.3. Overexpression of MUC4/X promotes cell invasion and migration

WT-MUC4 has been associated with increased invasion and motility in various malignancies including PC [7,34]. To analyze the effect of MUC4/X overexpression on cell invasion and migration, we performed a Boyden chamber assay as well as a wound healing assay. As seen in Fig. 3a, the number of invasive cells were significantly higher upon MUC4/X overexpression in MIAPaCa and AsPC-1 cells than with the control cells ($p < 0.005$, $p < 0.05$). The wound healing assay also revealed significantly enhanced wound closure by MUC4/X-OE PC cells compared to control cells ($p < 0.005$) (Supplementary Fig. S3a–b). Overall, overexpression of MUC4/X notably the enhanced invasive and migratory capability of PC cells.

Given that the TR domain is a heavily *O*-glycosylated domain of MUC4, its absence may influence the ability of MUC4 to interact with ECM [19]. Thus, we next examined how MUC4/X potentiates PC cell adherence to ECM proteins such as fibronectin, vitronectin, laminin, collagen IV, and collagen I. Both MUC4/X-OE and control PC cells were plated onto various ECM proteins coated 96-well plate. A significant increase in cell adhesion ($p < 0.001$) was observed on laminin, vitronectin, and fibronectin-coated wells by MUC4/X-OE cells (MIAPaCa and AsPC-1) when compared to control cells (Fig. 3b–c).

To assess the molecular mechanisms for differential adhesion to ECM proteins and enhanced migration/invasion by MUC4/X-OE cells, we examined the impact of MUC4/X overexpression on integrin-β1. Integrin-β1 was chosen as it is a known ligand for fibronectin, vitronectin, collagen IV and collagen I [35]. Our results revealed increased expression of integrin-β1 in MUC4/X-OE cells when compared to controls in conjunction with FAK, a non-receptor protein-tyrosine kinase which is involved in cell proliferation, invasion, adhesion, and metastasis [36]. Moreover, integrin-β1 plays a role in cell survival primarily by phosphorylation of FAK [37]. To delineate the molecular pathways associated with increased migration and invasion of PC cell upon MUC4/X overexpression, we evaluated its effect on the FAK/ERK signaling pathway. We observed increased expression of integrin-β1, phosphorylated FAK and ERK in MIAPaCa-MUC4/X and AsPC-1-MUC4/X cells as compared to control cells (Fig. 3d), signifying that MUC4/X might facilitate the invasive and metastatic potential of PC cells through the integrin-β1/FAK/ERK pathway. Additionally, since our EdU cell proliferation assay showed higher EdU incorporation which is generally incorporated in DNA synthesis S phase, we also analyzed the expression of cyclin A2, a well-established cyclin that promotes entry into S-phase and also considered as cell proliferation marker [38,39]. Corroborating with our *in vitro* data from the EdU cell proliferation assay, overexpression of MUC4/X in both PC cell lines elevated the expression of cyclin A2 (Fig. 3d). Overall, our results demonstrate that MUC4/X overexpression modulates oncogenic molecules and its downstream signaling to exacerbate the PC phenotype.

To better understand the underlying mechanism of MUC4/X tumorogenic potential, microarray analysis was performed in MIAPaCa-MUC4/X and control MIAPaCA-EV cells. Our results revealed ≥2-fold upregulation of CD44, Sortilin 2, Coronin 2B, integrin-α6, integrin-α3, and Interferon α4 (IFN-α4) in MIAPaCa-MUC4/X cells compared to vector control cells (Supplementary Fig. S4a). A full list of up- and down-regulated (≥2-fold) genes is provided in Supplementary Table S2. Indeed, validation of up-regulated genes from the microarray data using qPCR verified > 2-fold increase of CD44, Sortilin 2, Coronin 2B, integrin-α6, integrin-α3, IFN-α4, and MUC4 (Supplementary Fig. S4a–b). MUC4 showed a 44-fold up-regulation in the microarray analysis, resulting from the overexpression of MUC4/X as Human Gene 2.0 ST does not contain splicing probe, and MIAPaCa has a very low basal expression of WT-MUC4 (Supplementary Fig. S4b). Among the upre-gulated genes, CD44 and various integrins have been shown to be involved in promoting the tumorigenic potential of PC [40,41]. Moreover, CD44 has been associated with increased motility, adhesion, and chemoresistance in other malignancies [41]. Ingenuity Pathway Analysis (IPA) showed enrichment of ephrin receptor signaling and the axonal guidance pathway in the MIAPaCA-MUC4/X cells (Supplementary Fig. S4c). These have been implicated as critical pathways in PC tumorigenesis in previous studies [42,43].

3.4. MUC4/X overexpression fosters tumorigenicity in vivo

In vitro studies of MUC4/X-OE PC cells showed higher proliferative and invasive potential when compared to control cells. To ascertain whether the overexpression of MUC4/X can promote PC tumor growth and metastasis, we orthotopically implanted (2.5×10^5 cells in 50 μl of PBS) MIAPaCa-MUC4/X cells or control MIAPaCa-EV cells into the pancreas of

athymic nude mice (MIAPaCa-EV, n = 7, and MIAPaCa-MUC4/X, n = 8). At 50 days post-implantation, we euthanized the mice and observed that tumors formed by MIAPaCa-MUC4/X PC cells were significantly larger (average weight of 931 ± 291.69 mg) in comparison to the control cells (566 ± 178.38 mg) indicating that MUC4/X overexpression is involved in exacerbating PC tumorigenicity ($p < 0.05$) (Fig. 4a–b). Our IHC analysis of tumor tissues using anti-FLAG antibody confirmed maintenance of MUC4/X overexpression during tumor growth and metastasis (Fig. 4c). We also observed higher Ki-67, and integrin-β1 expression in MUC4/X-OE xenograft tumors (Fig. 4c). Furthermore, all the mice (8/8) implanted with MUC4/X-OE PC cells developed metastasis in distant organs, including diaphragm, spleen, and intestine (Supplementary Fig. S5). Interestingly, significant metastasis to peritoneal cavity (6/8), liver (5/8), kidney (5/8), mesenteric cavity (5/8) and stomach (2/8) was observed compared to control mice (peritoneal 1/7, liver 1/7, kidney 1/7, mesenteric cavity 0/7, and stomach 1/7) (Fig. 4d and Supplementary Fig. S5). Metastasis to the ovary (2/8), cecum (1/8), colon (1/8), and bladder (1/8) was exclusively observed in MUC4/X-OE cell-bearing mice (Fig. 4d and Supplementary Fig. S5). Our results suggest the involvement of MUC4/X in tumor growth and distant metastasis.

3.5. MUC4/X increases the adhesive capability to peritoneal LP9/TERT-1 cells

Peritoneal metastasis in PC reflects a devastating form of cancer progression that is intensely complex [44]. Probable mechanisms behind this fatal metastasis is augmented expression of adhesion molecules and integrin's, specifically integrin-β1, which play a significant role to help the cancer cells to attach to distant mesothelium [44]. As orthotopic transplantation of MIAPaCa-MUC4/X cells resulted in significant metastasis to the peritoneal cavity and increased expression of integrin-β1, we investigated whether MUC4/X-OE increases the adhesion capability of PC cells to immortalized peritoneal LP9/TERT-1 cells. To mimic the *in vivo* conditions where tumor cells would face the surface of the peritoneum, we coated 96 well plate with immortalized LP9/TERT-1 peritoneal cells follow by subsequent incubation with tumor cells (control and MUC4/X-OE) on top of the mesothelial monolayer for 5 h. Interestingly, MIAPaCa-MUC4/X (30%, $p < 0.05$) and AsPC-1-MUC4/X (60%, $p < 0.005$) cells significantly adhered to the mono-layer of LP9/TERT-1 as compared to control cells (Fig. 4e). These results suggested that MUC4/X plays a significant role in metastasizing PC cells to the peritoneum.

3.6. Overexpression of MUC4/X in the presence of endogenous MUC4, promotes cell proliferation, adhesion, and invasion

Both PC patient tissue samples, as well as PC cell lines, showed concomitant expression of MUC4 and its splice variant MUC4/X (Fig. 1e, Supplementary Fig. S1a and b). Earlier, MUC4 was shown to enhance proliferation, migration, and invasion of PC cells [8,19,34,45]. We were interested if the concomitant expression of WT-MUC4 and MUC4/X can synergistically enhance the tumorigenic properties of PC cells, or if their expression is redundant for cells.

To explore the explicit function of MUC4/X in PC, a tet-on inducible system was developed (Fig. 5a). Conditional activation of MUC4/X expression by doxycycline allowed us to decipher a gain of function of MUC4/X, in the presence of WT-MUC4.

Immunofluorescence and immunoblotting showed robust MUC4/X protein expression after 48 h of doxycycline treatment (Fig. 5b). Induction of MUC4/X didn't change the expression of WT-MUC4 (Fig. 5b). Thymidine analog EdU incorporation assay revealed that induction of MUC4/X in Capan-1 cells resulted in higher cell proliferation compared to doxycycline-negative Capan-1 cells (Fig. 5c, $p < 0.05$). Induction of MUC4/X also resulted in a significant increase in cell adhesion to ECM proteins such as laminin, collagen, and fibronectin (Fig. 5d, $p < 0.005$), as well as increased cell invasion ($p < 0.05$) as observed *via* Boyden chamber assay (Fig. 5e). Overexpression of MUC4/X did not change the expression of WT-MUC4, suggesting that MUC4/X overexpression mediates the phenomena of increased cell proliferation, invasion, and adhesion to ECM. Given that we observed MUC4/X overexpression in MIAPaCa, and AsPC-1 cell lines upregulated integrin-β1 and its downstream signaling molecules, we next sought to analyze their differential expression in tet-on inducible Capan-1 cell lines, in the presence of abundant expression of WT-MUC4. In concordance with the above-mentioned findings, doxycycline-induced MUC4/X resulted in higher integrin-β1 expression and increased pFAK, pERK and cyclin A2 expression in the presence of WT-MUC4 (Fig. 5f). This result suggested that conditional induction of MUC4/X in a WT-MUC4 expressing PC cell line, phenocopied the characteristics of MUC4/X in a WT-MUC4 negative cell line, emphasizing its tumorigenic role independent of WT-MUC4 expression.

4. Discussion

Transmembrane mucin MUC4 has previously been implicated in oncogenesis by initiating signaling *via* interaction and stabilization of HER2 [34]. Importantly, in the context of adhesion, the highly glycosylated TR domain of MUC4 has been hypothesized to interfere with tumor cell interaction with extracellular matrix (ECM) proteins, in part by blocking accessibility of integrins to ECM ligands sterically [19]. It has also been shown that a nonglycosylated TR of MUC1 facilitates attachment of tumor cells to the ECM to establish metastatic foci [46]. In addition, MUC1 without a TR domain displayed an aggressive PC phenotype *in vitro* and *in vivo* [47].

Apart from the TR domain, other functional domains of MUC4 has also been associated with invasion and metastasis of PC. Earlier studies from our group have suggested that the NIDO domain of MUC4, a domain similar to the G1 domain of a basement membrane nidogen (entactin), plays a critical role in invasion and metastasis. Deletion of NIDO domain from MUC4 decreased PC cells' invasion and metastasis [24]. Moreover, Tang et al. showed deletion of the adhesion-associated domain of MUC4 (AMOP domain) reduced invasion and metastasis of PC cells [48].

Overall, transmembrane mucins, with their various unique domains, are implicated in invasion and metastasis of tumor cells. Tumor cell invasion and metastasis is a complex process involving a delicate balance between adhesion and detachment of cancer cells with the ECM. This is initiated by dissemination of cancer cells from primary location followed by intravasation and subsequent extravasation through endothelial cells or lymphatics, to colonize distant organs [49]. Considering the significant role of MUC4 and its domains in intensifying PC malignant phenotype, the present study explored the biological significance

of MUC4/X, a splice variant that sans the heavily *O*-glycosylated TR domain of MUC4, on PC cells capability to adhere, invade, and metastasize.

MUC4/X is considered as a unique isoform of WT-MUC4, not only for lacking the TR domain, but also because of its adhesion-related functional attributes which are supposedly more accessible to the ECM due to the absence of steric hindrance by *O*-glycosylated TR domain. To comprehend the contribution of the TR domain deficient MUC4/X, we explored the interaction of MUC4/X overexpressing cells with various ECM components. ECM is a dense viscoelastic latticework composed of collagen, laminins, fibronectin, vitronectin, and different linker proteins (*i.e.* nidogen and entactin) which connect collagens with other proteins [50]. Cells can perceive direct or indirect signaling from the ECM by interacting with different ECM proteins [51,52]. Moreover, integrins can link the ECM to the intracellular actin cytoskeleton to commence intracellular signaling events by elevating gene expression involved in cell proliferation, survival, and migration [52]. In this regard, it has previously been shown that overexpression of MUC1 and MUC4 inhibit integrin-ECM interaction [19]. Of note, earlier studies utilizing a microarray of PC cell lines with a MUC1-TR-deleted construct, revealed upregulation of integrin-β5 [47]. In corroboration with this, our microarray data showed the upregulation of integrins (subunit α3 and α6) and CD44 in MUC4/X-OE PC cells.

Interestingly, knockdown of the integrin-β1 subunit reduced cell adhesion to ECM proteins and decreased PC tumor growth and metastasis [53]. Hence, we investigated the expression of integrin-β1, a binding partner of integrin α3 and α6, in MUC4/X overexpressing cells as well as in an inducible system. Surprisingly both showed upregulation of the β1 subunit of integrin. Integrin-β1 has been observed to play an essential role in cell adhesion, proliferation, and metastasis [35,53–55]. Notably, collagen (types I, III, and IV), fibronectin and laminin are known ligands for integrin-β1 [35]. The interactions between integrin-β1 and laminin are crucial for cell survival through FAK signaling [37]. Moreover, adhesion of cancer cells to ECM incites the intracellular signaling cascade for cell proliferation and invasion *via* integrin-β1/FAK/ERK signaling [56]. In the present study, we observed a similar phenomenon for MUC4/X, which promoted pancreatic malignancy by activating the integrin-β1/FAK/ERK pathway.

Peritoneal metastasis is one of the most frequent and deadly forms of PC metastasis [57]. Pancreatic tumors with peritoneal metastasis are highly resistant to chemotherapies with very poor patient survival (≤12 weeks). Moreover, the presence of peritoneal carcinomatosis has been associated with the development of intestinal obstruction, massive ascites, and malnutrition and is unfortunately associated with ~22% of patients morbidities [58]. In our orthotopic transplantation studies for MUC4/X, we observed significant metastasis to the liver and peritoneum. Though the mechanism for peritoneal carcinomatosis is still obscure, integrin-ECM interaction between tumor and mesothelial cells is considered as an early event in this process [59]. Evidenced by in-tegrin-β1 in ovarian carcinoma cells being associated with adhesion of ovarian carcinoma cells to mesothelial cells [30]. Our cell adhesion study revealed that MUC4/X overexpression resulted in significant adhesion to fibronectin, vitronectin, and laminin. It was shown earlier that LP9/TERT-1 mesothelial cell line expresses collagen types I, III, and IV, fibronectin and laminin [30]. Henceforth, we

evaluated adhesion ability of MUC4/X-OE cell to LP9/TERT-1 mesothelial cells. Results from peritoneal cell adhesion assay suggested that MUC4/X-OE cells have higher adherence to immortalized LP9/TERT-1 peritoneal cells as compared to control. We hypothesize that upregulation of in-tegrin-β1 by MUC4/X, and the higher adhesion capacity of MUC4/X-OE cells to the ECM proteins overexpressed in peritoneal cells, are the causative factors for enhanced adhesion and increased metastasis to peritoneum by MUC4/X-OE cells [30].

Considering the differential affinity of MUC4/X toward ECM proteins and WT-MUC4 as mentioned in earlier published reports, we speculate that they may either synergistically or reciprocally function at various stages of tumor development by potentiating invasion, adhesion and metastasis phenomena to drive PC malignancy. MUC4/X over-expression also resulted in increased cell proliferation in part by up-regulating cyclin A2, a mammalian A-type cyclin which is responsible for initiation and progression of DNA replication and G1-S phase transition and is considered a proliferation marker [38,39,60]. Similar to our study, cyclin A2 overexpression has also been observed in multiple malignancies including breast, prostate, colorectal and PC. It has been shown to contribute to the invasion, metastasis and tumorigenesis of these various cancers [61,62].

We observed concomitant expression of WT-MUC4 and MUC4/X in PC clinical samples. Interestingly, differential expression of MUC4/X was observed in poorly differentiated PC tumors. However, our studies were limited by lack of MUC4/X specific antibodies. In the future, development of such antibodies could lead to the evolution of improved biomarkers for PC detection. Further, to fully resolve the functional significance of MUC4/X, future orthotopic studies with an inducible system of MUC4/X in the background of WT-MUC4 would be carried out. A transgenic mouse model expressing human MUC4/X in the context of a pancreatic tumor will provide further insight into the functional relevance of this unique splice form.

Together, the results of this study propose the novel role of MUC4/X in PC cell proliferation, invasion, adhesion, and metastasis. The role of MUC4/X was investigated using *in vitro* and *in vivo* models and found to be mediated *via* upregulation of the integrin-β1/FAK/ERK pathway (Fig. 6). We have investigated the expression of MUC4/X in a cohort of patient tissues as well as cell lines, which suggest its aberrant upregulation in PC. The induced expression of MUC4/X in the presence of WT-MUC4 resulted in a high propensity of tumor cells to proliferate in addition to an increased capability of invasion, suggesting a non-redundant role of this splice variant. To our knowledge, this is the first report on the functional and mechanical role of MUC4/X, alone and with WT-MUC4, suggesting its role for conferring tumorigenic potential to PC. We have thus provided experimental evidence that WT-MUC4 and MUC4/X may be mutually beneficial for PC cells to develop and sustain an oncogenic phenotype at different stages of this lethal disease. Studies to determine the oncogenic role of a splice variant (in this case, MUC4/X) will help us to understand the complex molecular mechanism of PC and design much needed personalized therapeutic interventions.

Supplementary Material

Refer to Web version on PubMed Central for supplementary material.

Acknowledgments

The authors acknowledge the generous technical and management support of Mrs. Kavita Mallya. We also thank Ms. Janice A. Tayor and Mr. James R. Talaska, UNMC, for their technical assistance in confocal imaging and Ms. Melissa Holzapfel from Tissue Science facility, UNMC for assisting in tissue imaging and measuring the scale bar. We also thank Microarray Core Facility at the University of Kansas Medical Center (UKMC, USA) for their assistance in the microarray experiment. The UNMC RAP for pancreatic cancer is highly acknowledged. We also would like to thank Dr. Adrian E. Koesters, Research Editor at UNMC, for her substantial editorial contribution to this manuscript.

Grant support

This study was supported, in part, by grants from the NIH (RO1 CA210637, RO1CA206444, RO1 CA195586, O1 CA183459, UO1 CA200466, 1P50 CA127297 and R44 CA224619, R41CA213718) and a UNMC Graduate Fellowship to Rahat Jahan.

References

1. Siegel RL, Miller KD, Jemal A. Cancer statistics, 2018. CA Cancer J Clin. 2018; 68:7–30. [PubMed: 29313949]
2. Rahib L, Smith BD, Aizenberg R, Rosenzweig AB, Fleshman JM, Matrisian LM. Projecting cancer incidence and deaths to 2030: the unexpected burden of thyroid, liver, and pancreas cancers in the United States. Cancer Res. 2014; 74:2913–2921. [PubMed: 24840647]
3. Ladomery M. Aberrant alternative splicing is another hallmark of cancer. Int J Cell Biol. 2013; 2013:463786. [PubMed: 24101931]
4. Lee SC, Harn HJ, Lin TS, Yeh KT, Liu YC, Tsai CS, Cheng YL. Prognostic significance of CD44v5 expression in human thymic epithelial neoplasms. Ann Thorac Surg. 2003; 76:213–218. [PubMed: 12842543]
5. Takano S, Reichert M, Bakir B, Das KK, Nishida T, Miyazaki M, Heeg S, Collins MA, Marchand B, Hicks PD, Maitra A, Rustgi AK. Prrx1 isoform switching regulates pancreatic cancer invasion and metastatic colonization. Genes Dev. 2016; 30:233–247. [PubMed: 26773005]
6. Swartz MJ, Batra SK, Varshney GC, Hollingsworth MA, Yeo CJ, Cameron JL, Wilentz RE, Hruban RH, Argani P. MUC4 expression increases progressively in pancreatic intraepithelial neoplasia. Am J Clin Pathol. 2002; 117:791–796. [PubMed: 12090430]
7. Mukhopadhyay P, Lakshmanan I, Ponnusamy MP, Chakraborty S, Jain M, Pai P, Smith LM, Lele SM, Batra SK. MUC4 overexpression augments cell migration and metastasis through EGFR family proteins in triple negative breast cancer cells. PLoS One. 2013; 8:e54455. [PubMed: 23408941]
8. Rachagani S, Macha MA, Ponnusamy MP, Haridas D, Kaur S, Jain M, Batra SK. MUC4 potentiates invasion and metastasis of pancreatic cancer cells through stabilization of fibroblast growth factor receptor 1. Carcinogenesis. 2012; 33:1953–1964. [PubMed: 22791819]
9. Jonckheere N, Skrypek N, Van IS. Mucins and tumor resistance to chemotherapeutic drugs. Biochim Biophys Acta. 2014; 1846:142–151. [PubMed: 24785432]
10. Majhi PD, Lakshmanan I, Ponnusamy MP, Jain M, Das S, Kaur S, Shimizu ST, West WW, Johansson SL, Smith LM, Yu F, Rolle CE, Sharma P, Carey GB, Batra SK, Ganti AK. Pathobiological implications of MUC4 in non-small-cell lung cancer. J Thorac Oncol. 2013; 8:398–407. [PubMed: 23370366]
11. Singh AP, Chaturvedi P, Batra SK. Emerging roles of MUC4 in cancer: a novel target for diagnosis and therapy. Cancer Res. 2007; 67:433–436. [PubMed: 17234748]
12. Escande F, Lemaitre L, Moniaux N, Batra SK, Aubert JP, Buisine MP. Genomic organization of MUC4 mucin gene. Towards the characterization of splice variants. Eur J Biochem. 2002; 269:3637–3644. [PubMed: 12153560]

13. Chaturvedi P, Singh AP, Batra SK. Structure, evolution, and biology of the MUC4 mucin. FASEB J. 2008; 22:966–981. [PubMed: 18024835]
14. Moniaux N, Escande F, Batra SK, Porchet N, Laine A, Aubert JP. Alternative splicing generates a family of putative secreted and membrane-associated MUC4 mucins. Eur J Biochem. 2000; 267:4536–4544. [PubMed: 10880978]
15. Kumar S, Cruz E, Joshi S, Patel A, Jahan R, Batra SK, Jain M. Genetic variants of mucins: unexplored conundrum. Carcinogenesis. 2016; 38:671–679.
16. Zrihan-Licht S, Vos HL, Baruch A, Elroy-Stein O, Sagiv D, Keydar I, Hilkens J, Wreschner DH. Characterization and molecular cloning of a novel MUC1 protein, devoid of tandem repeats, expressed in human breast cancer tissue. Eur J Biochem. 1994; 224:787–795. [PubMed: 7925397]
17. Xie K, Zhi X, Tang J, Zhu Y, Zhang J, Li Z, Tao J, Xu Z. Upregulation of the splice variant MUC4/Y in the pancreatic cancer cell line MIA PaCa-2 potentiates proliferation and suppresses apoptosis: new insight into the presence of the transcript variant of MUC4. Oncol Rep. 2014; 31:2187–2194. [PubMed: 24676527]
18. Zhu Y, Zhang JJ, Liang WB, Zhu R, Wang B, Miao Y, Xu ZK. Pancreatic cancer counterattack: MUC4 mediates Fas-independent apoptosis of antigen-specific cytotoxic T lymphocyte. Oncol Rep. 2014; 31:1768–1776. [PubMed: 24534824]
19. Chaturvedi P, Singh AP, Moniaux N, Senapati S, Chakraborty S, Meza JL, Batra SK. MUC4 mucin potentiates pancreatic tumor cell proliferation, survival, and invasive properties and interferes with its interaction to extracellular matrix proteins. Mol Cancer Res. 2007; 5:309–320. [PubMed: 17406026]
20. Hollingsworth MA, Swanson BJ. Mucins in cancer: protection and control of the cell surface. Nat Rev Cancer. 2004; 4:45–60. [PubMed: 14681689]
21. Makiguchi Y, Hinoda Y, Imai K. Effect of MUC1 mucin, an anti-adhesion molecule, on tumor cell growth. Jpn J Cancer Res. 1996; 87:505–511. [PubMed: 8641988]
22. Komatsu M, Carraway CA, Fregien NL, Carraway KL. Reversible disruption of cell-matrix and cell-cell interactions by overexpression of sialomucin complex. J Biol Chem. 1997; 272:33245–33254. [PubMed: 9407114]
23. Dickson MA, Hahn WC, Ino Y, Ronfard V, Wu JY, Weinberg RA, Louis DN, Li FP, Rheinwald JG. Human keratinocytes that express hTERT and also bypass a p16(INK4a)-enforced mechanism that limits life span become immortal yet retain normal growth and differentiation characteristics. Mol Cell Biol. 2000; 20:1436–1447. [PubMed: 10648628]
24. Senapati S, Gnanapragassam VS, Moniaux N, Momi N, Batra SK. Role of MUC4-NIDO domain in the MUC4-mediated metastasis of pancreatic cancer cells. Oncogene. 2012; 31:3346–3356. [PubMed: 22105367]
25. Moniaux N, Chaturvedi P, Varshney GC, Meza JL, Rodriguez-Sierra JF, Aubert JP, Batra SK. Human MUC4 mucin induces ultra-structural changes and tumorigenicity in pancreatic cancer cells. Br J Cancer. 2007; 97:345–357. [PubMed: 17595659]
26. Gomez-Martinez M, Schmitz D, Hergovich A. Generation of stable human cell lines with Tetracycline-inducible (Teton) shRNA or cDNA expression. J Vis Exp. 2013:e50171. [PubMed: 23486277]
27. Macha MA, Rachagani S, Qazi AK, Jahan R, Gupta S, Patel A, Seshacharyulu P, Lin C, Li S, Wang S, Verma V, Kishida S, Kishida M, Nakamura N, Kibe T, Lydiatt WM, Smith RB, Ganti AK, Jones DT, Batra SK, Jain M. Afatinib radiosensitizes head and neck squamous cell carcinoma cells by targeting cancer stem cells. Oncotarget. 2017; 8:20961–20973. [PubMed: 28423495]
28. Lakshmanan I, Rachagani S, Hauke R, Krishn SR, Paknikar S, Seshacharyulu P, Karmakar S, Nimmakayala RK, Kaushik G, Johansson SL, Carey GB, Ponnusamy MP, Kaur S, Batra SK, Ganti AK. MUC5AC interactions with integrin beta4 enhances the migration of lung cancer cells through FAK signaling. Oncogene. 2016; 35:4112–4121. [PubMed: 26751774]
29. Lee JG, Ahn JH, Jin Kim T, Ho Lee J, Choi JH. Mutant p53 promotes ovarian cancer cell adhesion to mesothelial cells via integrin beta4 and Akt signals. Sci Rep. 2015; 5:12642. [PubMed: 26223322]

30. Lessan K, Aguiar DJ, Oegema T, Siebenson L, Skubitz AP. CD44 and beta1 integrin mediate ovarian carcinoma cell adhesion to peritoneal mesothelial cells. Am J Pathol. 1999; 154:1525–1537. [PubMed: 10329605]

31. Das S, Rachagani S, Torres-Gonzalez MP, Lakshmanan I, Majhi PD, Smith LM, Wagner KU, Batra SK. Carboxyl-terminal domain of MUC16 imparts tumorigenic and metastatic functions through nuclear translocation of JAK2 to pancreatic cancer cells. Oncotarget. 2015; 6:5772–5787. [PubMed: 25691062]

32. Moniaux N, Varshney GC, Chauhan SC, Copin MC, Jain M, Wittel UA, Andrianifahanana M, Aubert JP, Batra SK. Generation and characterization of anti-MUC4 monoclonal antibodies reactive with normal and cancer cells in humans. J Histochem Cytochem. 2004; 52:253–261. [PubMed: 14729877]

33. Rachagani S, Senapati S, Chakraborty S, Ponnusamy MP, Kumar S, Smith LM, Jain M, Batra SK. Activated KrasG(1)(2)D is associated with invasion and metastasis of pancreatic cancer cells through inhibition of E-cadherin. Br J Cancer. 2011; 104:1038–1048. [PubMed: 21364589]

34. Chaturvedi P, Singh AP, Chakraborty S, Chauhan SC, Bafna S, Meza JL, Singh PK, Hollingsworth MA, Mehta PP, Batra SK. MUC4 mucin interacts with and stabilizes the HER2 oncoprotein in human pancreatic cancer cells. Cancer Res. 2008; 68:2065–2070. [PubMed: 18381409]

35. Bodary SC, McLean JW. The integrin beta 1 subunit associates with the vitronectin receptor alpha v subunit to form a novel vitronectin receptor in a human embryonic kidney cell line. J Biol Chem. 1990; 265:5938–5941. [PubMed: 1690718]

36. Bouchard V, Demers MJ, Thibodeau S, Laquerre V, Fujita N, Tsuruo T, Beaulieu JF, Gauthier R, Vezina A, Villeneuve L, Vachon PH. Fak/Src signaling in human intestinal epithelial cell survival and anoikis: differentiation state-specific uncoupling with the PI3-K/Akt-1 and MEK/Erk pathways. J Cell Physiol. 2007; 212:717–728. [PubMed: 17443665]

37. Santos AR, Corredor RG, Obeso BA, Trakhtenberg EF, Wang Y, Ponmattam J, Dvoriantchikova G, Ivanov D, Shestopalov VI, Goldberg JL, Fini ME, Bajenaru ML. beta1 integrin-focal adhesion kinase (FAK) signaling modulates retinal ganglion cell (RGC) survival. PLoS One. 2012; 7:e48332. [PubMed: 23118988]

38. Gu WW, Lin J, Hong XY. Cyclin A2 regulates homologous recombination DNA repair and sensitivity to DNA damaging agents and poly(ADP-ribose) polymerase (PARP) inhibitors in human breast cancer cells. Oncotarget. 2017; 8:90842–90851. [PubMed: 29207607]

39. Meloche S, Pouyssegur J. The ERK1/2 mitogen-activated protein kinase pathway as a master regulator of the G1- to S-phase transition. Oncogene. 2007; 26:3227–3239. [PubMed: 17496918]

40. Grzesiak JJ, Ho JC, Moossa AR, Bouvet M. The integrin-extracellular matrix axis in pancreatic cancer. Pancreas. 2007; 35:293–301. [PubMed: 18090233]

41. Li XP, Zhang XW, Zheng LZ, Guo WJ. Expression of CD44 in pancreatic cancer and its significance. Int J Clin Exp Pathol. 2015; 8:6724–6731. [PubMed: 26261555]

42. Lisabeth EM, Falivelli G, Pasquale EB. Eph receptor signaling and ephrins, Cold Spring Harb. Perspect Biol. 2013; 5

43. Biankin AV, Waddell N, Kassahn KS, Gingras MC, Muthuswamy LB, Johns AL, Miller DK, Wilson PJ, Patch AM, Wu J, Chang DK, Cowley MJ, Gardiner BB, Song S, Harliwong I, Idrisoglu S, Nourse C, Nourbakhsh E, Manning S, Wani S, Gongora M, Pajic M, Scarlett CJ, Gill AJ, Pinho AV, Rooman I, Anderson M, Holmes O, Leonard C, Taylor D, Wood S, Xu Q, Nones K, Fink JL, Christ A, Bruxner T, Cloonan N, Kolle G, Newell F, Pinese M, Mead RS, Humphris JL, Kaplan W, Jones MD, Colvin EK, Nagrial AM, Humphrey ES, Chou A, Chin VT, Chantrill LA, Mawson A, Samra JS, Kench JG, Lovell JA, Daly RJ, Merrett ND, Toon C, Epari K, Nguyen NQ, Barbour A, Zeps N, I. Australian Pancreatic, N. Cancer Genome. Kakkar F, Wu Zhao YQ, Wang M, Muzny DM, Fisher WE, Brunicardi FC, Hodges SE, Reid JG, Drummond J, Chang K, Han Y, Lewis LR, Dinh H, Buhay CJ, Beck T, Timms L, Sam M, Begley K, Brown A, Pai D, Panchal A, Buchner N, De Borja R, Denroche RE, Yung CK, Serra S, Onetto N, Mukhopadhyay D, Tsao MS, Shaw PA, Petersen GM, Gallinger S, Hruban RH, Maitra A, Iacobuzio-Donahue CA, Schulick RD, Wolfgang CL, Morgan RA, Lawlor RT, Capelli P, Corbo V, Scardoni M, Tortora G, Tempero MA, Mann KM, Jenkins NA, Perez-Mancera PA, Adams DJ, Largaespada DA, Wessels LF, Rust AG, Stein LD, Tuveson DA, Copeland NG, Musgrove EA, Scarpa A, Eshleman JR, Hudson TJ, Sutherland RL, Wheeler DA, Pearson JV, McPherson JD, Gibbs RA, Grimmond SM. Pancreatic cancer

genomes reveal aberrations in axon guidance pathway genes. Nature. 2012; 491:399–405. [PubMed: 23103869]

44. Kusamura S, Baratti D, Zaffaroni N, Villa R, Laterza B, Balestra MR, Deraco M. Pathophysiology and biology of peritoneal carcinomatosis. World J Gastrointest Oncol. 2010; 2:12–18. [PubMed: 21160812]
45. Jahan R, , Kaur S, , Macha MA, , Batra SK. Mucins (MUCs), Encyclopedia of Signaling Molecules Springer; New York: 2016 114
46. Ciborowski P, Finn OJ. Non-glycosylated tandem repeats of MUC1 facilitate attachment of breast tumor cells to normal human lung tissue and immobilized extracellular matrix proteins (ECM) in vitro: potential role in metastasis. Clin Exp Metastasis. 2002; 19:339–345. [PubMed: 12090474]
47. Kohlgraf KG, Gawron AJ, Higashi M, Meza JL, Burdick MD, Kitajima S, Kelly DL, Caffrey TC, Hollingsworth MA. Contribution of the MUC1 tandem repeat and cytoplasmic tail to invasive and metastatic properties of a pancreatic cancer cell line. Cancer Res. 2003; 63:5011–5020. [PubMed: 12941828]
48. Tang J, Zhu Y, Xie K, Zhang X, Zhi X, Wang W, Li Z, Zhang Q, Wang L, Wang J, Xu Z. The role of the AMOP domain in MUC4/Y-promoted tumour angiogenesis and metastasis in pancreatic cancer. J Exp Clin Cancer Res. 2016; 35:91. [PubMed: 27287498]
49. Bendas G, Borsig L. Cancer cell adhesion and metastasis: selectins, integrins, and the inhibitory potential of heparins. Int J Cell Biol. 2012; 2012:676731. [PubMed: 22505933]
50. Barczyk M, Carracedo S, Gullberg D. Integrins. Cell Tissue Res. 2010; 339:269–280. [PubMed: 19693543]
51. Lu P, Weaver VM, Werb Z. The extracellular matrix: a dynamic niche in cancer progression. J Cell Biol. 2012; 196:395–406. [PubMed: 22351925]
52. Stupack DG, Cheresh DA. Get a ligand, get a life: integrins, signaling and cell survival. J Cell Sci. 2002; 115:3729–3738. [PubMed: 12235283]
53. Grzesiak JJ, Tran Cao HS, Burton DW, Kaushal S, Vargas F, Clopton P, Snyder CS, Deftos LJ, Hoffman RM, Bouvet M. Knockdown of the beta(1) integrin subunit reduces primary tumor growth and inhibits pancreatic cancer metastasis. Int J Cancer. 2011; 129:2905–2915. [PubMed: 21491421]
54. Bouchard V, Harnois C, Demers MJ, Thibodeau S, Laquerre V, Gauthier R, Vezina A, Noel D, Fujita N, Tsuruo T, Arguin M, Vachon PH. B1 integrin/Fak/Src signaling in intestinal epithelial crypt cell survival: integration of complex regulatory mechanisms. Apoptosis. 2008; 13:531–542. [PubMed: 18322799]
55. Hazlehurst LA, Damiano JS, Buyuksal I, Pledger WJ, Dalton WS. Adhesion to fibronectin via beta1 integrins regulates p27kip1 levels and contributes to cell adhesion mediated drug resistance (CAM-DR). Oncogene. 2000; 19:4319–4327. [PubMed: 10980607]
56. Reddig PJ, Juliano RL. Clinging to life: cell to matrix adhesion and cell survival. Cancer Metastasis Rev. 2005; 24:425–439. [PubMed: 16258730]
57. Deeb A, Haque SU, Olowokure O. Pulmonary metastases in pancreatic cancer, is there a survival influence? J Gastrointest Oncol. 2015; 6:E48–E51. [PubMed: 26029466]
58. Thomassen I, Lemmens VE, Nienhuijs SW, Luyer MD, Klaver YL, de Hingh IH. Incidence, prognosis, and possible treatment strategies of peritoneal carcinomatosis of pancreatic origin: a population-based study. Pancreas. 2013; 42:72–75. [PubMed: 22850624]
59. Kaur S, Kenny HA, Jagadeeswaran S, Zillhardt MR, Montag AG, Kistner E, Yamada SD, Mitra AK, Lengyel E. (beta)3-integrin expression on tumor cells inhibits tumor progression, reduces metastasis, and is associated with a favorable prognosis in patients with ovarian cancer. Am J Pathol. 2009; 175:2184–2196. [PubMed: 19808644]
60. Arsic N, Bendris N, Peter M, Begon-Pescia C, Rebouissou C, Gadea G, Bouquier N, Bibeau F, Lemmers B, Blanchard JM. A novel function for Cyclin A2: control of cell invasion via RhoA signaling. J Cell Biol. 2012; 196:147–162. [PubMed: 22232705]
61. Casimiro MC, Crosariol M, Loro E, Li Z, Pestell RG. Cyclins and cell cycle control in cancer and disease. Genes Cancer. 2012; 3:649–657. [PubMed: 23634253]
62. Ito Y, Takeda T, Wakasa K, Tsujimoto M, Okada M, Matsuura N. Expression of the G2-M modulators in pancreatic adenocarcinoma. Pancreatology. 2002; 2:138–145. [PubMed: 12123094]

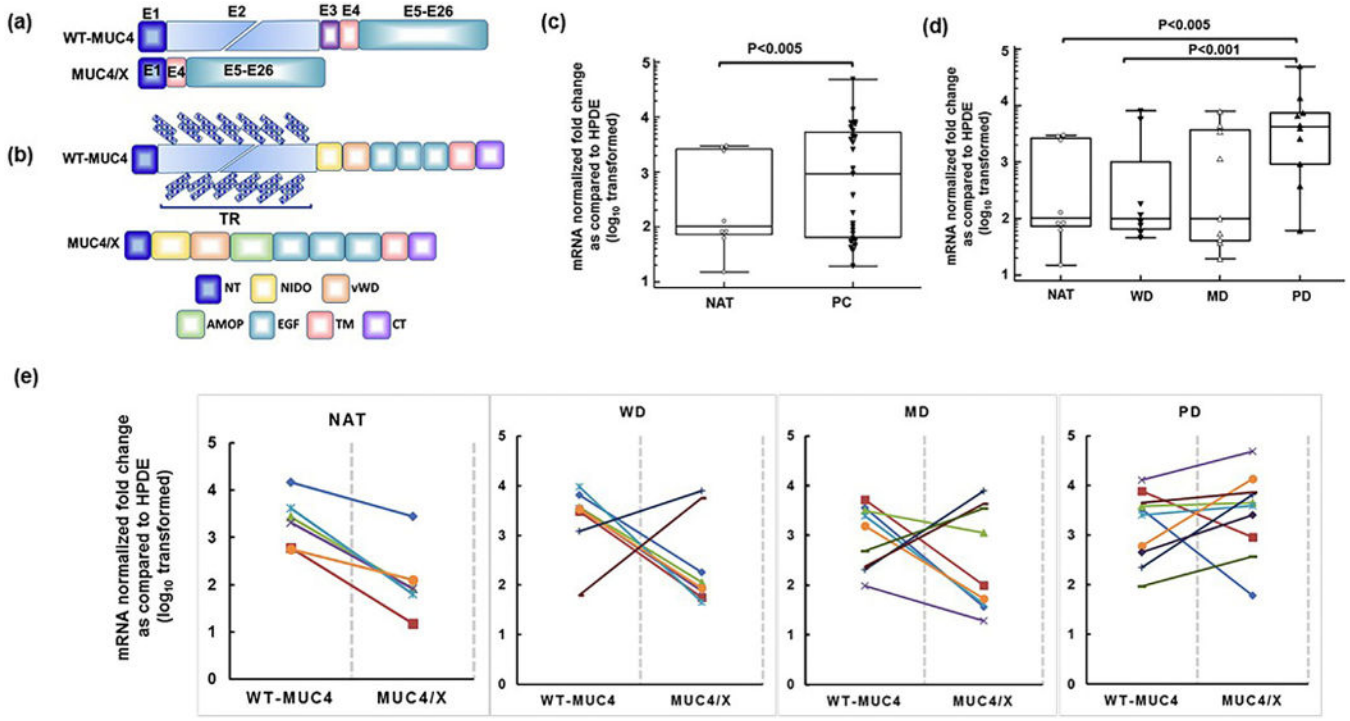

Fig. 1.

Expression of MUC4/X and wild-type (WT)-MUC4 mRNA in pancreatic cancer (PC) clinical samples and normal adjacent pancreatic tissues (NAT). (a) Schematic diagram of WT-MUC4 and MUC4/X mRNA structure. The WT-MUC4 is comprised of 26 exons while splice variant MUC4/X is devoid of exons 2 and 3. Exons are represented by box. (b) Schematic diagram of the domain structure of WT-MUC4 and MUC4/X. WT-MUC4 is a transmembrane mucin characterized by the presence of multiple domains including N-terminal (NT), Tandem Repeat (TR), Nidogen like (NIDO), Adhesion-associated domain in mucin MUC4 and other protein (AMOP), von Willebrand D (vWD), Epidermal Growth Factor (EGF), transmembrane (TM), and cytoplasmic (CT) domain. The unique splice variant, MUC4/X, is characterized by the presence of all domains of WT-MUC4 except the heavily glycosylated and polymorphic TR domain. Diagonally placed blue checker boxes represent *O*-glycosylation within the TR domain present in WT-MUC4. (c–d) Box and whisker plots are representing MUC4/X mRNA fold change ($\log_{10}$ transformed) in PC tissues and normal tissues adjacent to tumor (NAT) by qPCR and ΔΔCt method. (c) Significantly, elevated expression of MUC4/X was observed in pancreatic tumor tissues in comparison to NAT tissues ($p < 0.005$). (d) The qPCR analysis of MUC4/X mRNA expression levels in pancreatic NAT, well-differentiated (WD), moderately-differentiated (MD), and poorly-differentiated (PD) cases. Elevated expression of MUC4/X was observed in PD pancreatic tumors in comparison to NAT ($p < 0.005$) as well as WD tumors ($p < 0.001$). Two-tailed Student's *t*-test was used to determine the statistical difference between two groups. The circle represents individual mRNA expression in NAT tissues whereas triangle represents PC cases. The interquartile range (IQR) for MUC4/X expression is presented by box and whisker plot (horizontal line represents the 25th percentile, median and 75th percentile and whisker represents 5th and 95th percentile). (e) Line diagram is

representing mRNA fold change (log10 transformed) of both WT-MUC4-and MUC4/X in PC tissues and normal tissues adjacent to tumor by qPCR and ΔΔCt methods in NAT, WD, MD, and PD groups. Each line represents individual patient data for WT-MUC4 and MUC4/X where the left and right endpoint represent fold change of WT-MUC4 and MUC4/X expression respectively. β-actin was used as an internal control to normalize the expression of respective gene, and normal human pancreatic ductal epithelial (HPDE) cell line mRNA expression levels were used as calibrant control for determining fold change across patient groups. Y-Axis represent value as fold change (log10 relative quantification) relative to HPDE.

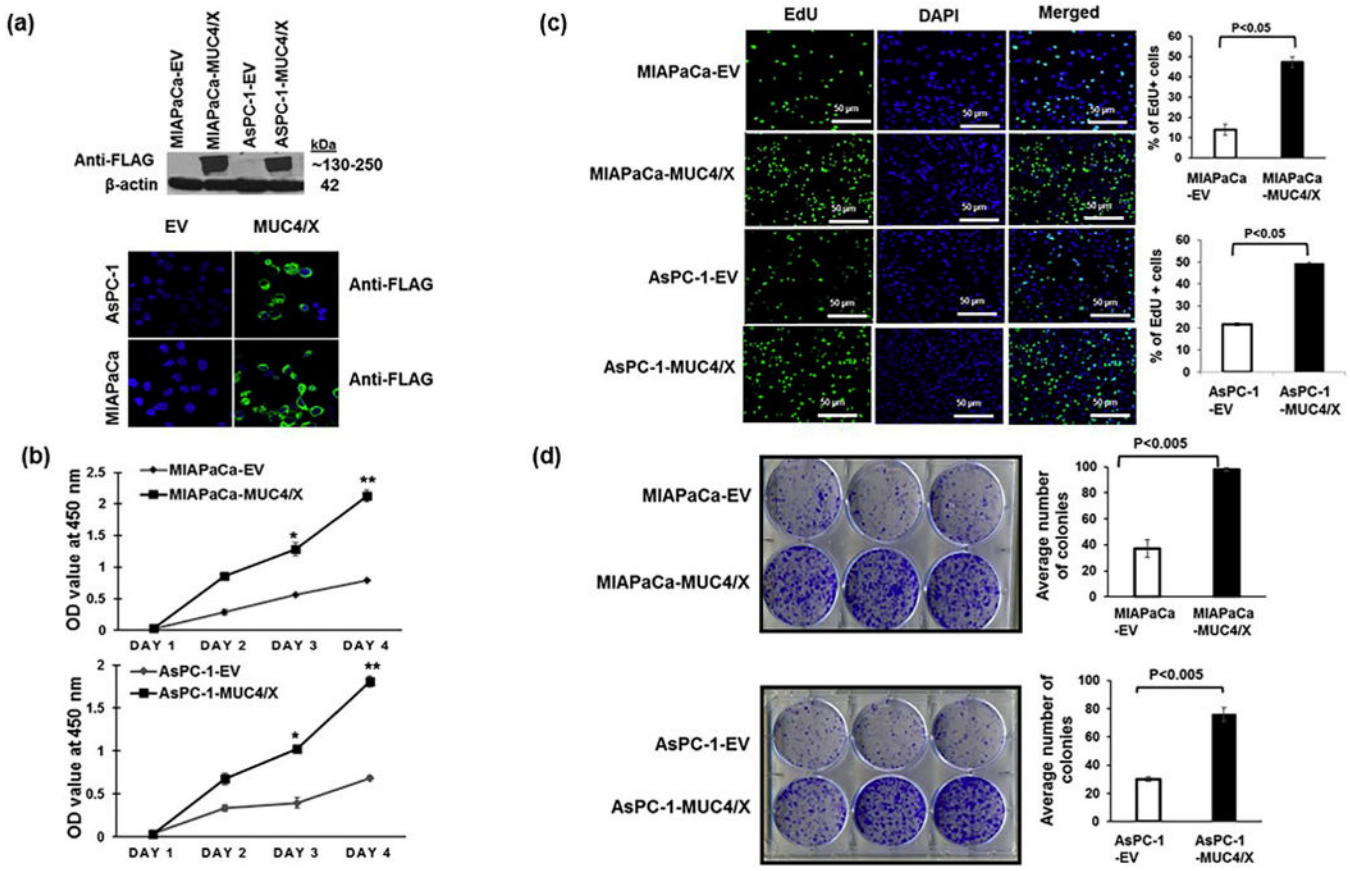

Fig. 2.

Functional implications of overexpression of the MUC4/X on PC cell proliferation and colony formation. (a) MUC4/X was cloned into the N-terminus FLAG-tagged, and the C-terminus HA-tagged p3XFLAG-CMV™-9 vector followed by stable transfection into WT-MUC4 non-expression PC cell lines MIAPaCa and AsPC-1. (Upper panel) Immunoblot analyses using anti-FLAG antibody was performed to assess the expression of MUC4/X. MUC4/X overexpression was observed in stably transfected MIAPaCa-MUC4/X and AsPC-1-MUC4/X cells whereas no expression was detected in empty vector (EV) transfected cells. (Lower Panel) Immunofluorescence analyses for MUC4/X using anti-FLAG antibody showed expression of MUC4/X in MIAPaCa-MUC4/X, and AsPC-1-MUC4/X PC cells while no expression was observed in vector alone transfected cells. (b) MTT assay was performed to assess the impact of MUC4/X overexpression on cellular proliferation. Significant higher cell proliferation in MIAPaCa-MUC4/X and AsPC-1-MUC4/X cell lines were observed as compared to vector transfected control cells at 3rd and 4th days (MIAPaCa-EV/AsPC-1-EV) ($^{**}p < 0.01$, $^{*}p < 0.05$). Line diagram represents the OD value at 450 nm (mean ± SD, n = 3). (c) EdU cell proliferation assay was performed to assess the impact of MUC4/X overexpression on PC cell proliferation. MUC4/X-OE cells had a higher number of EdU positive proliferating (green fluorescent) cells as compared to control vector transfected cells ($p < 0.05$) after 24 h of incubation with EdU. Nuclei staining with DAPI represents total number of cells. Accompanying bar diagram demonstrates the quantitative measurement for percentages of EdU positive green fluorescent cells (mean ±

SD, n = 3). (d) Colony forming assay suggested MUC4/X-transfected MIAPaCa and AsPC-1 cells formed significantly greater number of colonies than the control cells ($p < 0.005$). The corresponding bar diagram represents quantitative analysis of an average number of colonies (mean ± SD, n = 3) observed per well of six-well plates. The two-tailed, unpaired *t*-test analyses was used to determine significance between two groups. These results suggest MUC4/X overexpression promotes cell proliferation and colony formation.

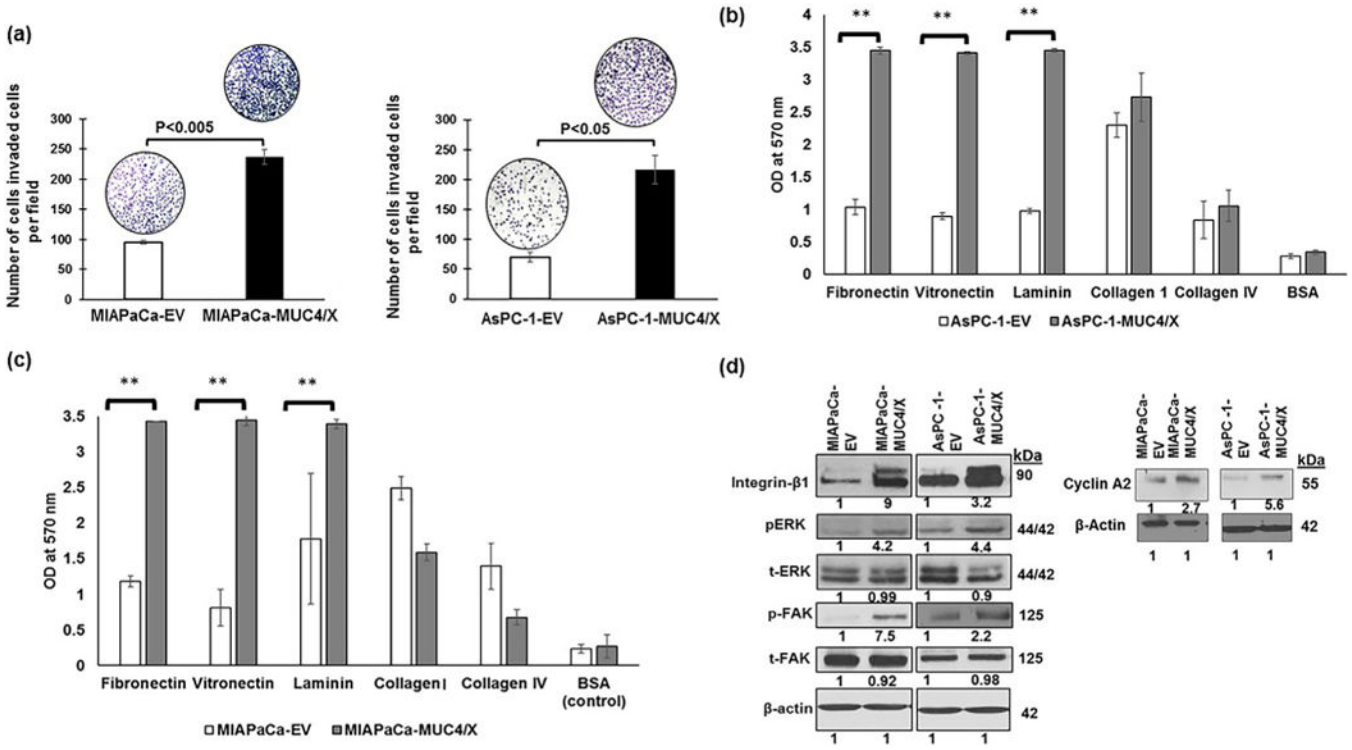

Fig. 3.

Functional and molecular implication of MUC4/X overexpression on PC cell. (a) Boyden chamber assay was performed to evaluate the impact of MUC4/X overexpression on invasive property of tumor cells. Higher number of invaded cells were observed in MUC4/X overexpressing MIAPaCa ($p < 0.005$) and AsPC-1 ($p < 0.05$) cells in comparison to control cells. Bar diagram represents the average number of invaded cells per field (mean ± SD, n = 5). (b–c) Cell attachment assay on ECM coated plate was performed to assess adhesion property of MUC4/X-OE and control cells. MUC4/X overexpression increased cell adhesion to extracellular matrix proteins including fibronectin, vitronectin, and laminin (**$p < 0.001$). For statistical significance comparison of two groups, a two-tailed, unpaired t-test was performed. Bar diagram represents mean OD value at 570 nm (mean ± SD, n = 3). BSA served as negative control for adhesion assay studies. (d) To analyze oncogenic signaling pathway activated by MUC4/X, we performed immunoblotting for integrin-β1, pFAK, tFAK (total FAK), pERK, tERK (total ERK) and cyclin A2. β-actin was used as a loading control. Fold change was assessed by quantitative analyses of immunoblotting results upon overexpression of MUC4/X as compared to control cells (represented by numerical value underneath immunoblot results). MUC4/X overexpression led to upregulation of integrin-β1, pFAK, and pERK in both MIAPaCa and AsPC-1 cell line. These results demonstrate that MUC4/X overexpression increased cell invasion and cell adhesion to ECM by modulating integrin-β1/FAK/ERK pathway.

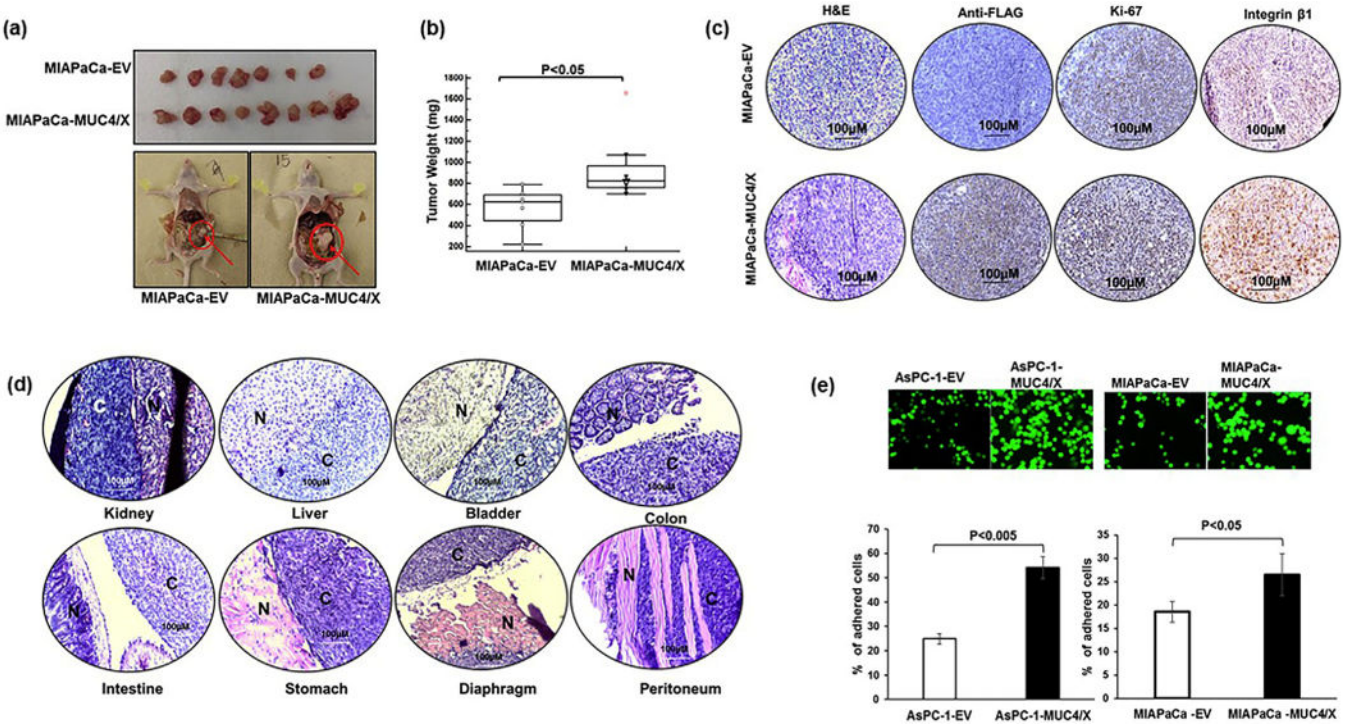

Fig. 4.

Effect of MUC4/X overexpression on tumor growth and metastasis *in vivo*. Orthotopic transplantation in the pancreas of nude mice was performed to evaluate the tumorigenic potential of MUC4/X *in vivo*. (a) MIAPaCa-EV and MIAPaCa-MUC4/X cells (2.5×10^5) were orthotopically implanted into the pancreas of nude mice (MIAPaCa-EV (n = 7), MIAPaCa-MUC4/X (n = 8)). Orthotropic implantation of MIAPaCa-MUC4/X cells shows increased tumor-forming ability as compared to the vector-transfected cells. Upper panel image represents extracted tumors from both control and MUC4/X overexpressed groups. The lower panel shows the anatomic image of tumor resection from control and MUC4/X-OE groups. (b) The tumors were excised from mice weighed and averaged; the box and whisker plot displays the tumor weights of mice from control and experimental groups. Mice that received MIAPaCa-MUC4/X cells manifest greater tumor weight compared to the mice which received MIAPaCa-EV cells ($p < 0.05$). The box and whisker plot represent the interquartile range (IQR) (horizontal line represents the 25th percentile, median and 75th percentile and whisker represents 5th and 95th percentile). The red dot represents outliers. Data were analyzed using two-tailed unpaired *t*-test to determine statistical significance. (c) H&E, as well as immunohistochemistry of FLAG (for assessing MUC4/X expression), Ki67, and integrin-β1 was performed on extracted tumor section. IHC revealed elevated level of MUC4/X, Ki67 and integrin-β1 in MIAPaCA-MUC4/X mice group in comparison to MIAPaCa-EV group. (d) Micrographs of H&E stained sections showed metastasis to kidney, intestine, colon, bladder, liver, stomach, diaphragm and peritoneum in the MIAPaCa-MUC4/X injected cells in nude animals. Scale bar is displayed in each image (100 μm). N represents the normal tissues of the organ whereas, C represents cancer cells in the same organ. (e) Representative immunofluorescent images from peritoneal adhesion assay are suggesting that AsPC-1-MUC4/X ($p < 0.005$) and MIAPaCa-MUC4/X ($p < 0.05$) cells have

higher cell adhesion to LP-9 peritoneal mesothelial monolayer as compared to control cells. Accompanying bar diagram represents the mean value of the percentage of cells (mean ± SD, n = 3) adhered to peritoneal cells. Data was analyzed using two-tailed unpaired *t*-test to determine significance. These results demonstrate that overexpression of MUC4/X promotes tumor growth and metastasis *in vivo*.

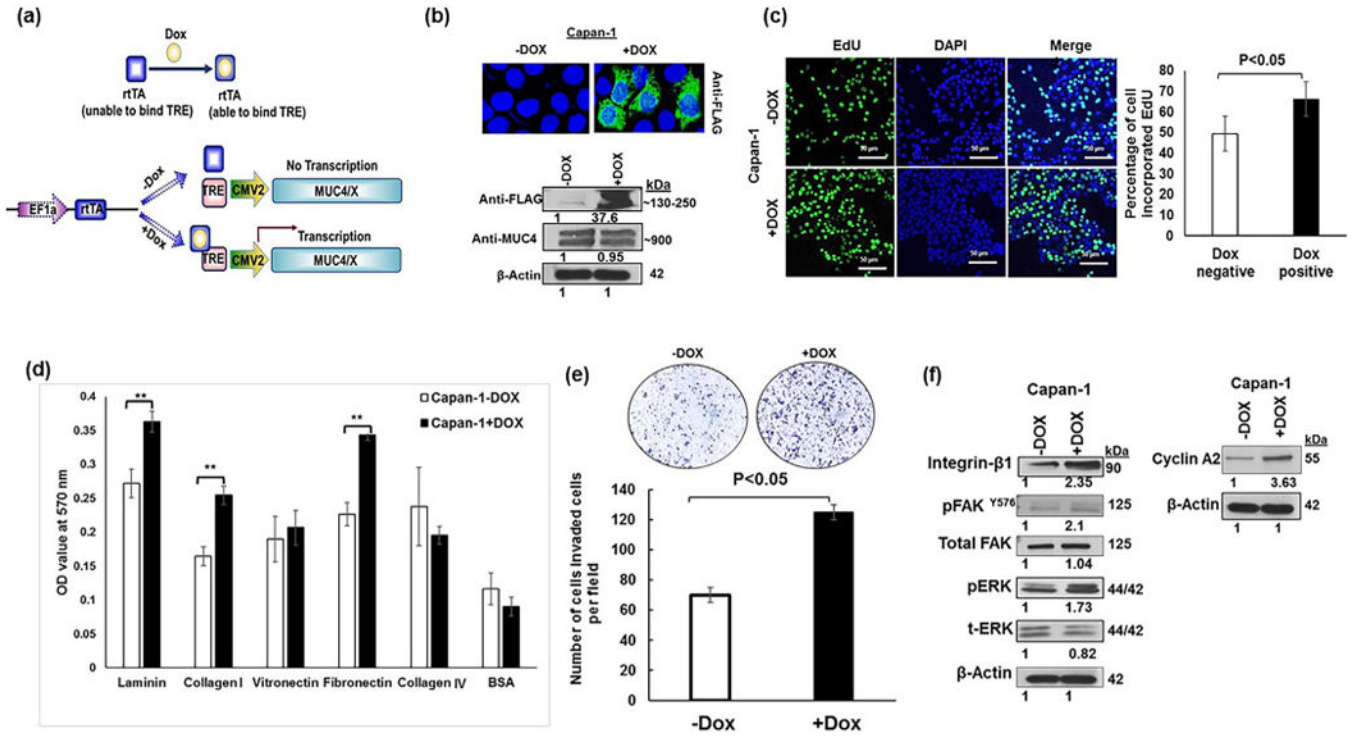

Fig. 5.

Mechanistic implication of MUC4/X in the background of WT-MUC4. (a) Schematic layout for MUC4/X induction in WT-MUC4 expressing PC cells. Upon doxycycline treatment, the conformational change of rtTA (reverse tetracycline-controlled transactivator) results in binding with TRE (Tet Response Element) which in-turn leads to induction of MUC4/X. (b) Immunoblotting (lower panel) and confocal images (upper panel) showing induction of MUC4/X expression upon doxycycline treatment in WT-MUC4 expressing Capan-1 cells. No alteration in the expression of WT-MUC4 was observed on induction of MUC4/X. (c) Doxycycline induction of MUC4/X resulted in higher cell proliferation within 24 h in the background of WT-MUC4 as indicated by EdU cell proliferation assay. Accompanying bar diagram shows an increase in the percentage of the proliferative cell upon MUC4/X induction ($p < 0.05$). (d) Induction of MUC4/X resulted in significantly higher cell adhesion to the ECM proteins (**$p < 0.005$). The corresponding bar diagram represents OD value (mean ± SD, n = 3). BSA served as a negative control. (e) Boyden Chamber assay is demonstrating that induction of MUC4/X in Capan-1 cell line resulted in higher number of invaded cells. Accompanying bar diagram represents the number of invaded cells per field (mean ± SD). (f) Western blots indicate that increased expression of integrin-β1, pFAK, pERK and cyclin A2 upon induction of MUC4/X in Capan-1 cells. β-actin was used as a loading control. Each blot represents the numerical fold change value upon overexpression of MUC4/X.

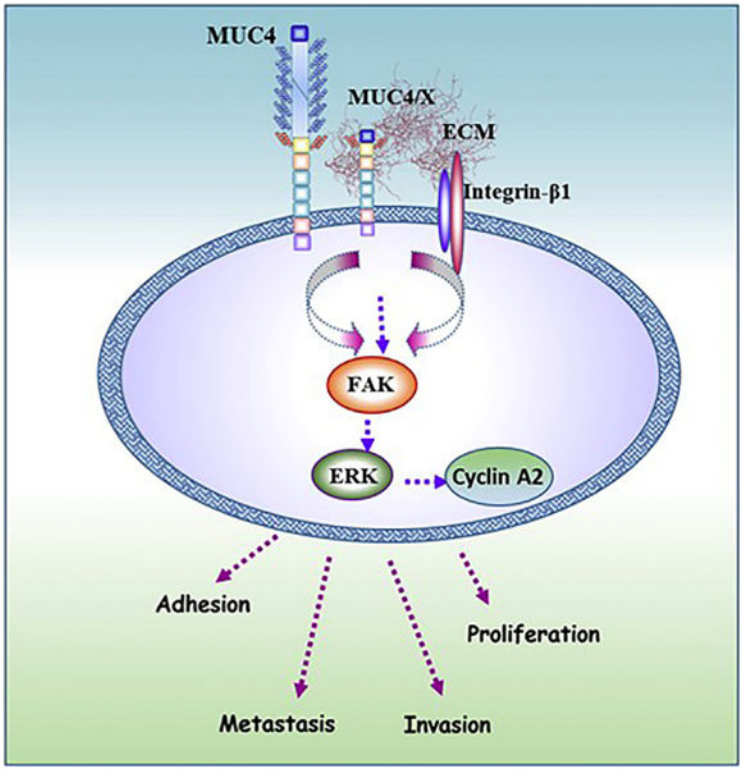

Fig. 6.

Molecular mechanism of MUC4/X mediated oncogenic signaling in PC tumorigenesis. Schematic diagram showing the oncogenic role of MUC4/X in PC. Ectopic expression of MUC4/X in PC cells resulted in elevated expression of integrin-β1 and increased adhesion to ECM thereby activating downstream FAK/ERK signaling along with cyclin A2 overexpression. Activation of this signaling cascade results in cell proliferation, adhesion, invasion, and metastasis. When the expression of MUC4/X is induced ectopically along with WT-MUC4, it also exhibited a similar aggressive oncogenic phenotype. Overall, overexpression of MUC4/X leads to enhanced aggressiveness of PC.